

SUPPLEMENTARY MATERIAL

Anti- β -amyloid Aggregation Activity of Enantiomeric Furolactone-type Lignans from *Archidendron clypearia* (Jack) I.C.N.

Yu-Xi Wang^{1a}, Bin Lin^{1b}, Le Zhou^a, Zhi-Yang Yan^a, Zhang Han^a, Xiao-Xiao Huang^{a,c,*},
Shao-Jiang Song^{a*}

^a *School of Traditional Chinese Materia Medica, Key Laboratory of Structure-Based Drug Design and Discovery, Ministry of Education, Shenyang Pharmaceutical University, Shenyang 110016, People's Republic of China*

^b *School of Pharmaceutical Engineering, Shenyang Pharmaceutical University, Shenyang 110016, People's Republic of China*

^c *Chinese People's Liberation Army 210 Hospital, Dalian 116021, People's Republic of China*

*Corresponding author.

E-mail addresses: xiaoxiao270@163.com (X.-X. Huang), songsj99@163.com. (S.-J. Song).

¹ These authors contributed equally to this work.

Anti- β -amyloid Aggregation Activity of Enantiomeric Furo lactone-type Lignans from *Archidendron clypearia* (Jack) I.C.N.

Abstract

The phytochemical investigation on the twigs and leaves of *Archidendron clypearia* (Jack) I.C.N. led to the isolation of three pairs of furo lactone-type lignans enantiomers, including a pair of new compounds (1*R*,5*S*,6*S*)-Kachiranol (**1a**) and (1*S*,5*R*,6*R*)-Kachiranol (**1b**) and four known compounds (**2a/2b** and **3a/3b**). Separation of the furo lactone-type lignans enantiomeric mixtures was achieved using chiral HPLC for the first time. Their structures were determined by spectroscopic analysis and comparison between the experimental and calculated electronic circular dichroism (ECD) spectra. All optical pure compounds were evaluated for their inhibitory effects on β -amyloid aggregation by ThT assay. Among them, the inhibitory activity of the compound **1b** (71.1 %) was higher than the positive control (61.0 %) and other compounds. In addition, molecular dynamics and molecular docking were employed to explore the binding relationship between the ligand and the receptor.

Keywords: *Archidendron clypearia* (Jack) I.C.N.; enantiomers; furo lactone-type lignans; $A\beta$ aggregation; molecular dynamics; molecular docking

Table of Contents

- Figure S1.** ^1H NMR spectrum (400 MHz, $\text{DMSO-}d_6$) of compound **1**
- Figure S2.** ^{13}C NMR spectrum (100 MHz, $\text{DMSO-}d_6$) of compound **1**
- Figure S3.** Key HMBC and NOESY correlations of compound **1**.
- Figure S4.** HMBC spectrum (600 MHz, $\text{DMSO-}d_6$) of compound **1**
- Figure S5.** HSQC spectrum (600 MHz, $\text{DMSO-}d_6$) of compound **1**
- Figure S6.** NOESY spectrum (600 MHz, $\text{DMSO-}d_6$) of compound **1**
- Figure S7.** Experimental and calculated ECD spectrum of compounds A: **1a/1b**, B: **2a/2b** and C: **3a/3b** in MeOH.
- Figure S8.** HRESIMS spectrum of compound **1**
- Figure S9.** A and C: H-bonding interactions of compounds **2a/2b** and $A\beta_{42}$ in docking models. B and D: 2D schematic diagram of compounds **2a/2b** and $A\beta_{42}$ in docking models.
- Figure S10.** A and C: H-bonding interactions of compounds **3a/3b** and $A\beta_{42}$ in docking models. B and D: 2D schematic diagram of compounds **3a/3b** and $A\beta_{42}$ in docking models.
- Figure S11.** Binding mode of compound **1b** depicted by 3D docking pose associated with amyloid beta fibril (2BEG).
- Figure S12.** Binding mode depicted by 2D view of ligand interaction diagram of associated with amyloid beta fibril (2BEG). (A-F: **1a-3b**)
- Figure S13.** The chiral resolution HPLC spectra of compounds **1a/1b**.
- Figure S14.** The chiral resolution HPLC spectra of compounds **2a/2b**.
- Figure S15.** The chiral resolution HPLC spectra of compounds **3a/3b**.

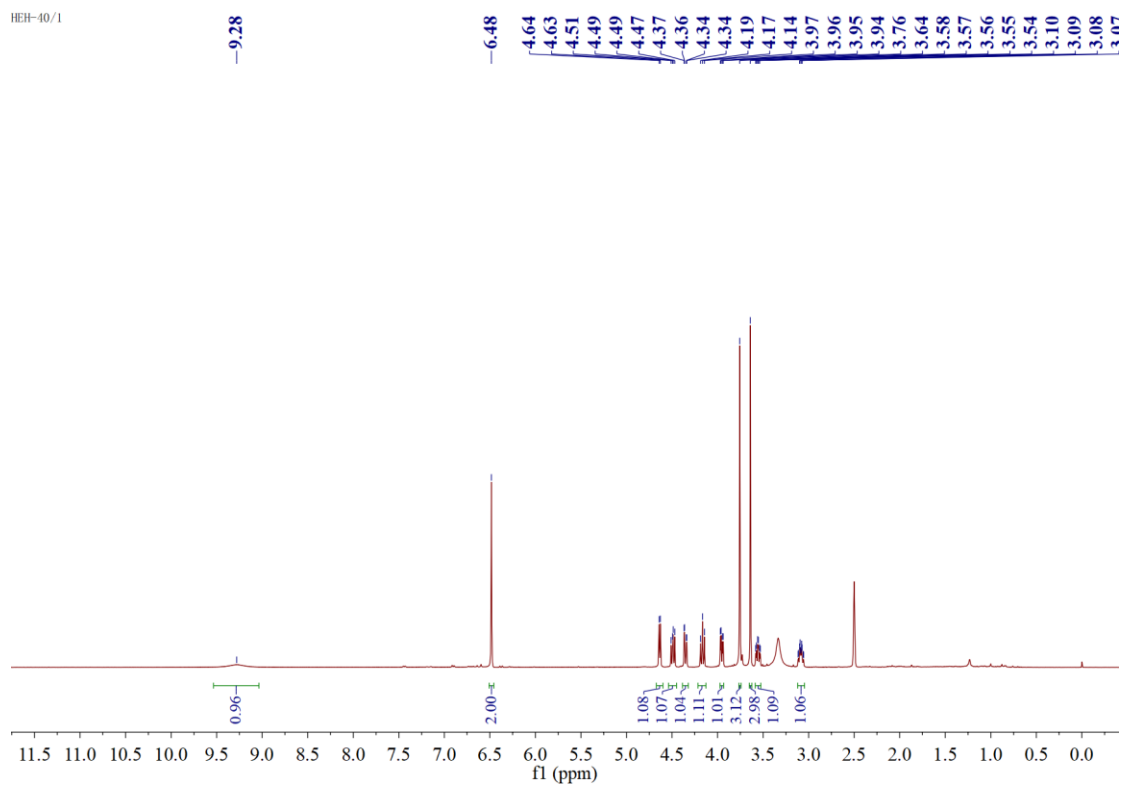


Figure S1. ^1H NMR spectrum (400 MHz, $\text{DMSO-}d_6$) of compound **1**

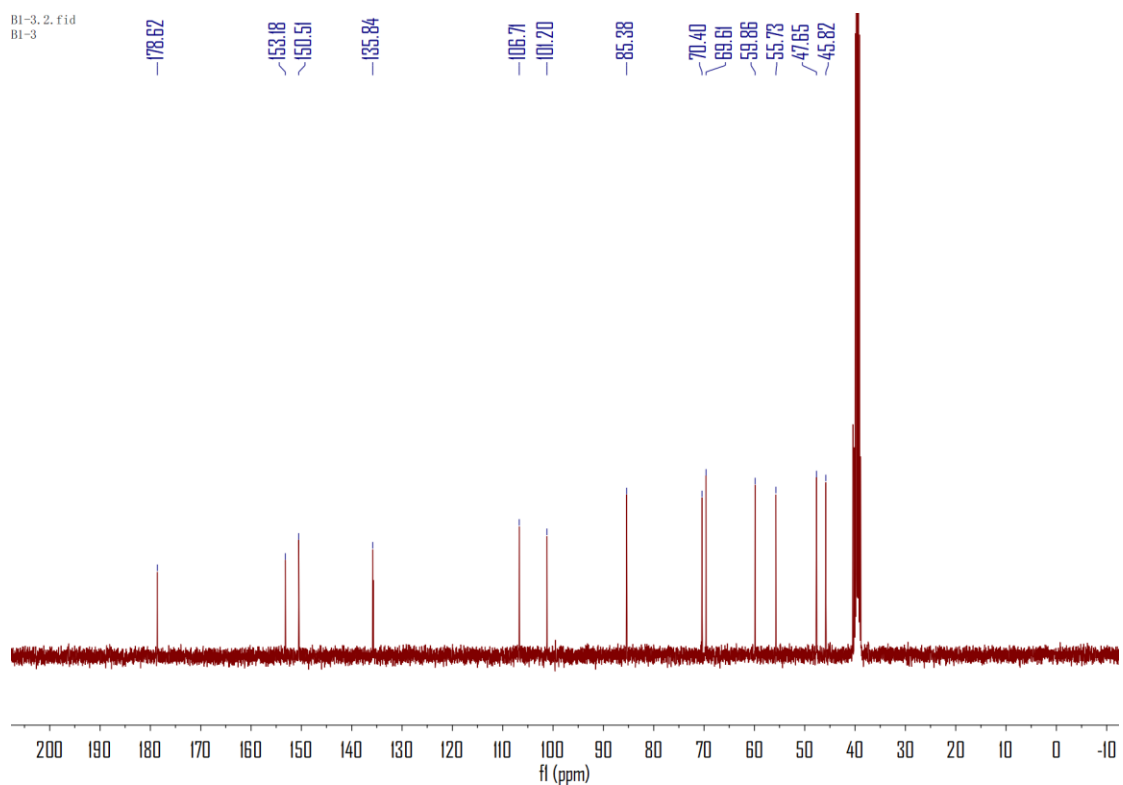


Figure S2. ^{13}C NMR spectrum (100 MHz, $\text{DMSO-}d_6$) of compound **1**

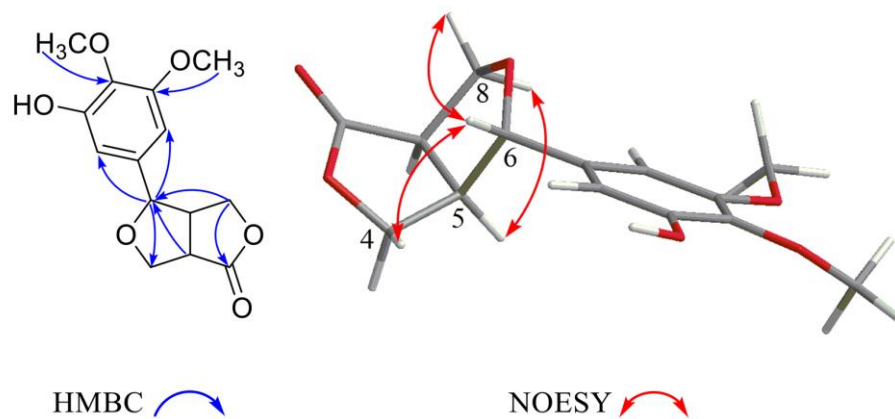


Figure S3. Key HMBC and NOESY correlations of compound **1**.

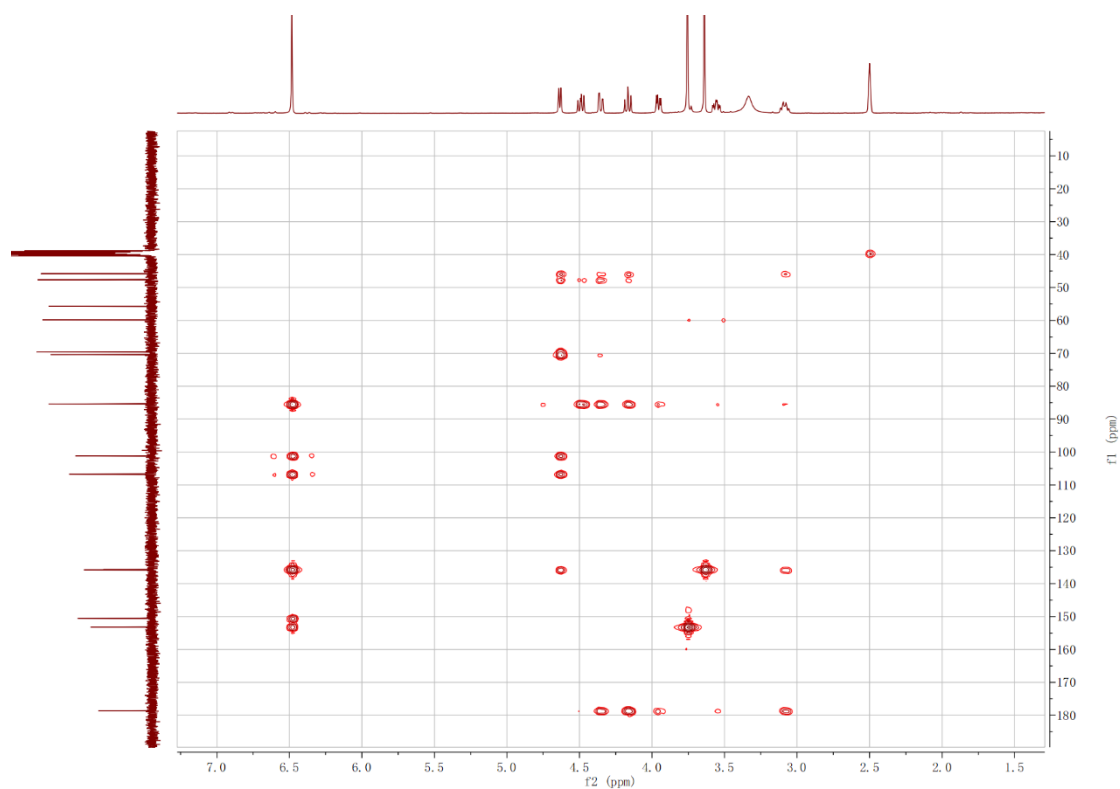


Figure S4. HMBC spectrum (600 MHz, DMSO- d_6) of compound **1**

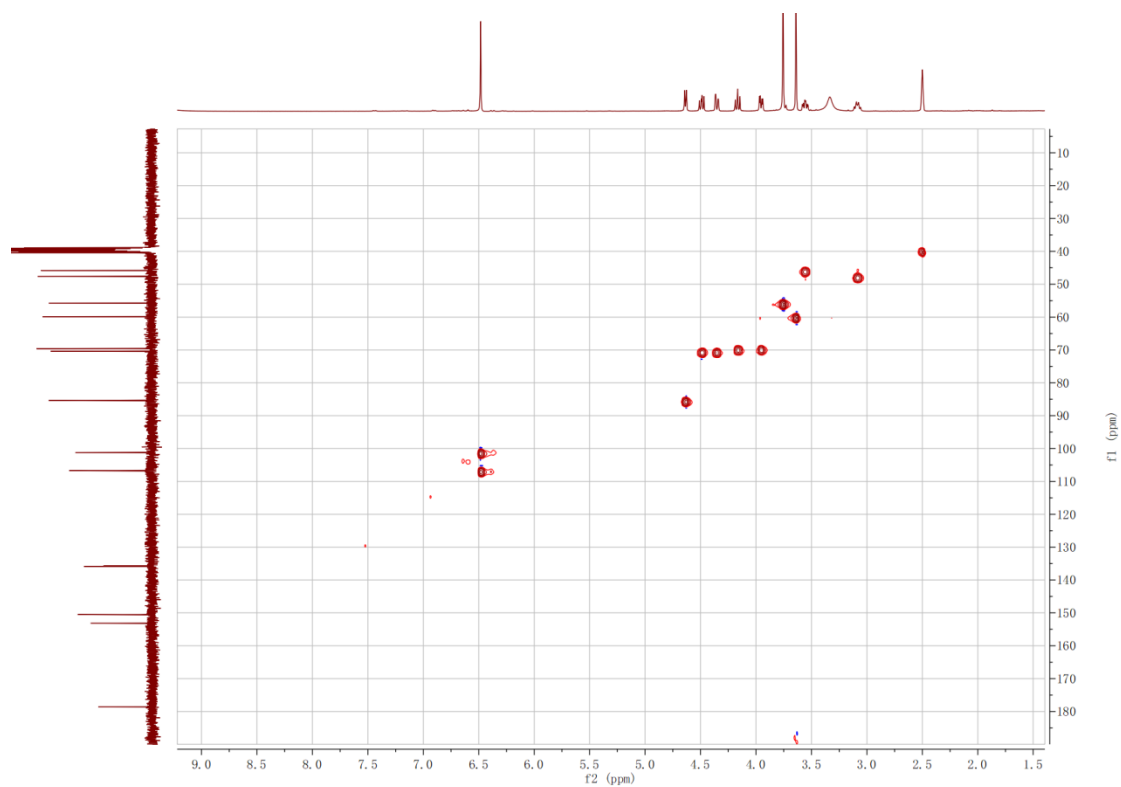


Figure S5. HSQC spectrum (600 MHz, DMSO- d_6) of compound **1**

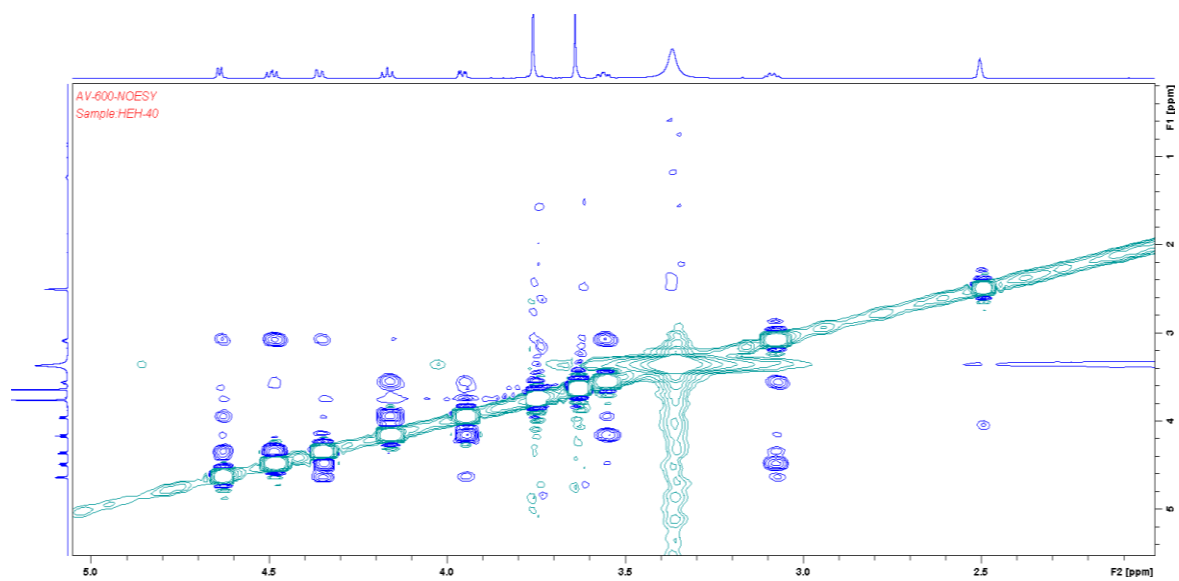


Figure S6. NOESY spectrum (600 MHz, DMSO- d_6) of compound **1**

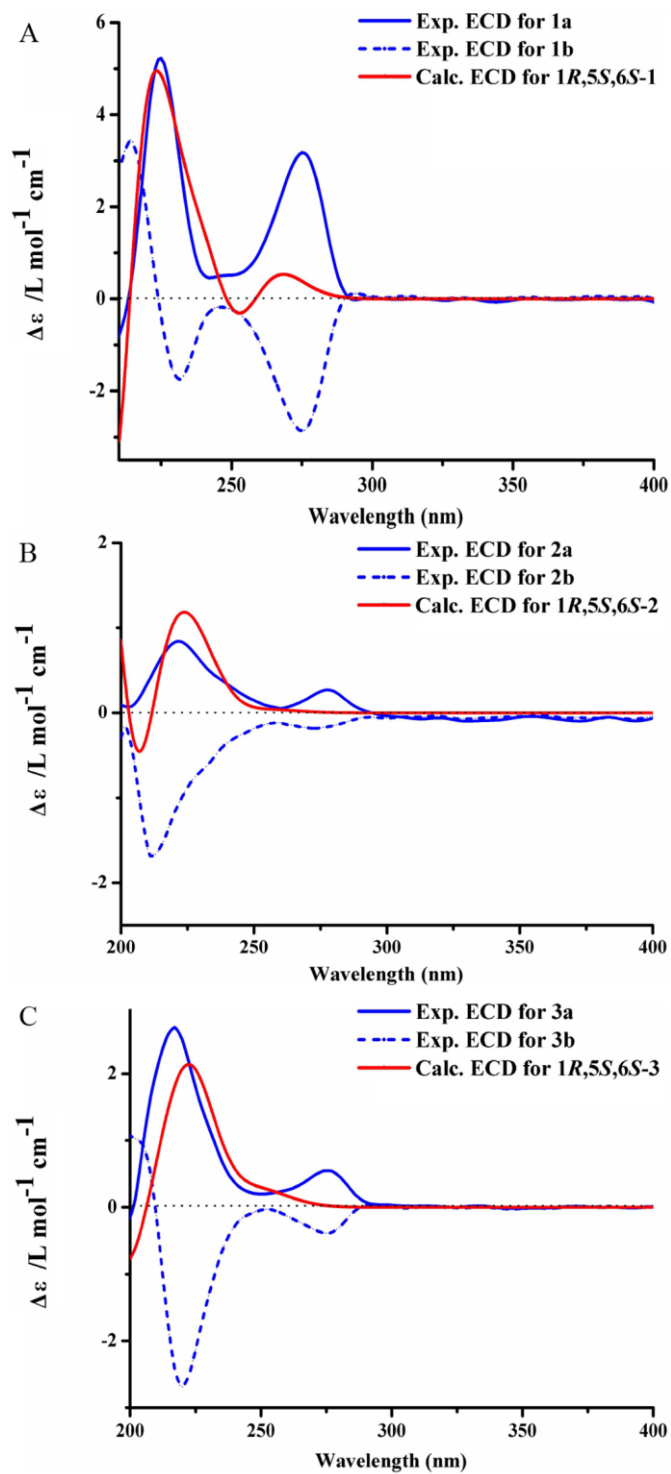


Figure S7. Experimental and calculated ECD spectrum of compounds A: **1a/1b**, B: **2a/2b** and C: **3a/3b** in MeOH.

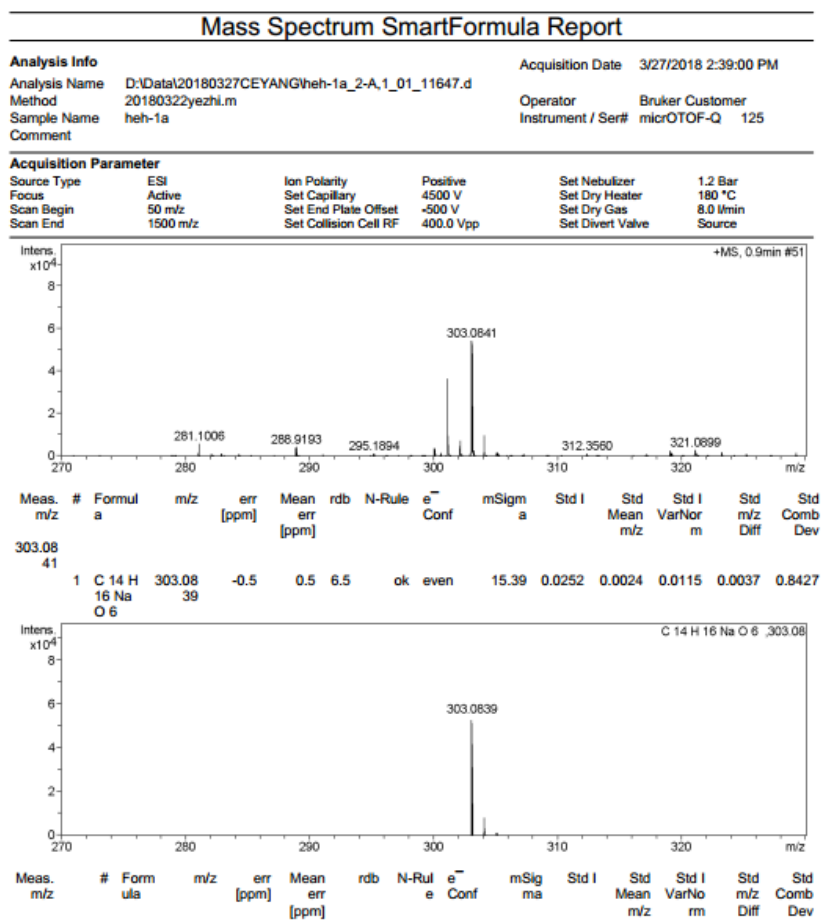


Figure S8. HRESIMS spectrum of compound **1**

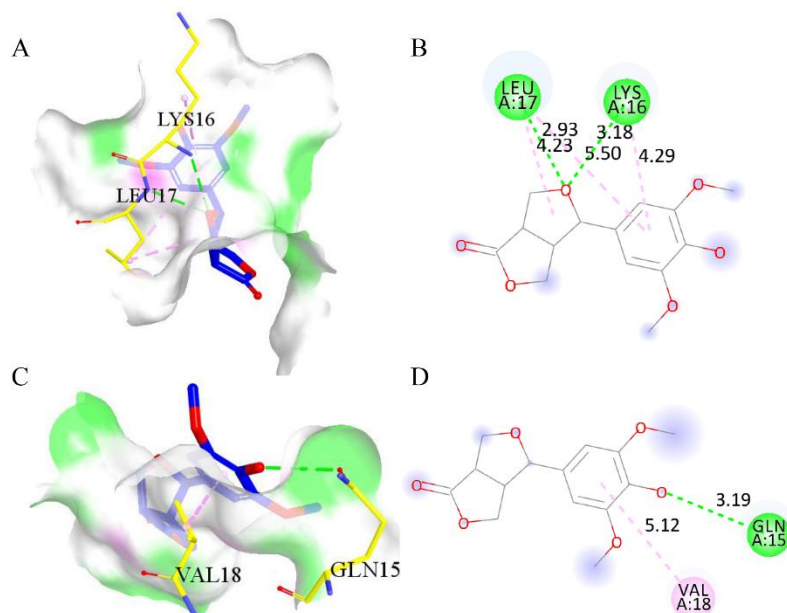


Figure S9. A and C: H-bonding interactions of compounds **2a/2b** and $A\beta_{42}$ in docking models. B and D: 2D schematic diagram of compounds **2a/2b** and $A\beta_{42}$ in docking models.

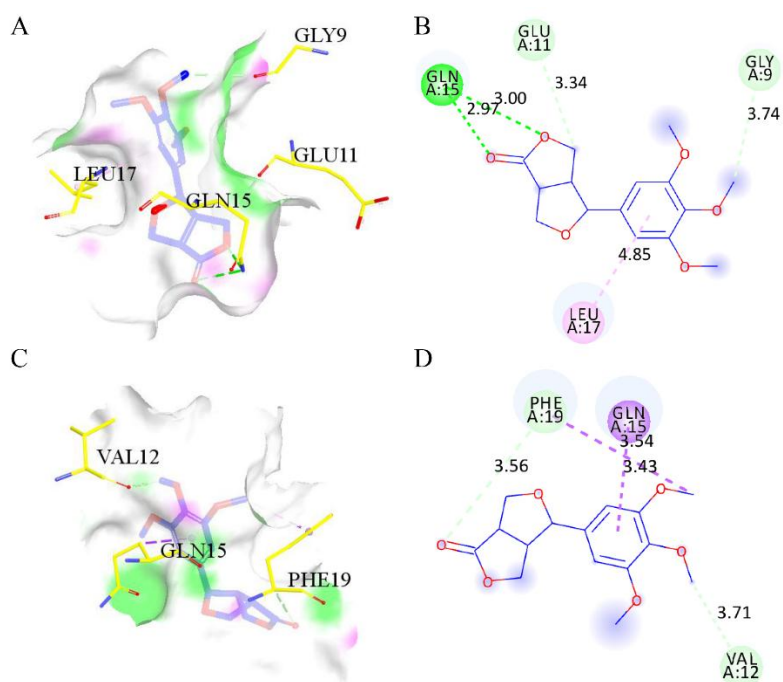


Figure S10. A and C: H-bonding interactions of compounds **3a/3b** and $A\beta_{42}$ in docking models. B and D: 2D schematic diagram of compounds **3a/3b** and $A\beta_{42}$ in docking models.

$A\beta$ fibrils are also important substrates in β -amyloid aggregation inhibitory activity assay. Therefore, we take this type of $A\beta_{42}$ for the docking study as a complement. The 3D docking pose was showed in Fig. R2. The 2D view of ligand interaction diagram between $A\beta$ fibrils and the molecules were similar to the single $A\beta$ poly-peptide used in our previous study (Fig. R3). In compounds 1a/1b, the C-3' hydroxyl groups were responsible for the main increase observed in potency. These interactions will decrease when the hydroxyl groups located in C-4' (2a/2b) or substituted by methoxy groups (3a/3b). The results were also matched well with ThT-based fluorometric assay.

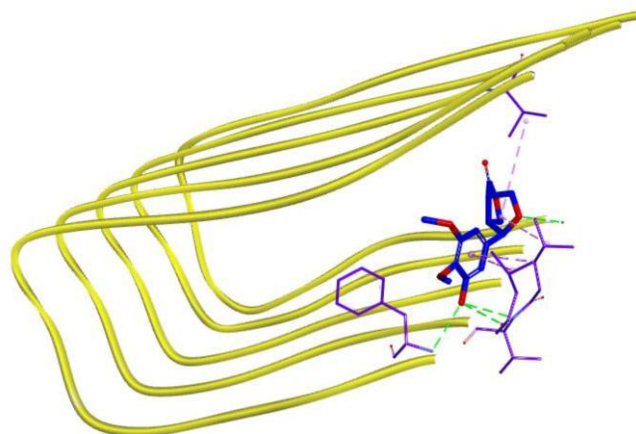


Figure S11. Binding mode of compound **1b** depicted by 3D docking pose associated with amyloid beta fibril (2BEG).

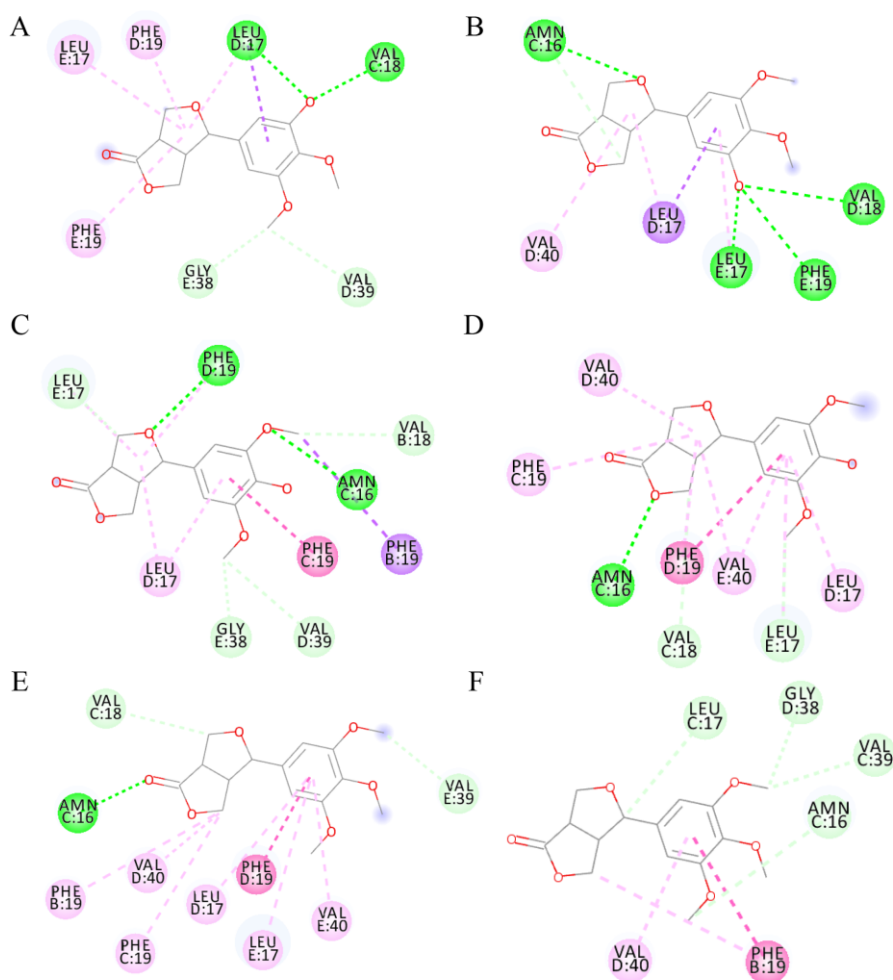


Figure S12. Binding mode depicted by 2D view of ligand interaction diagram of associated with amyloid beta fibril (2BEG). (A-F: **1a-3b**)

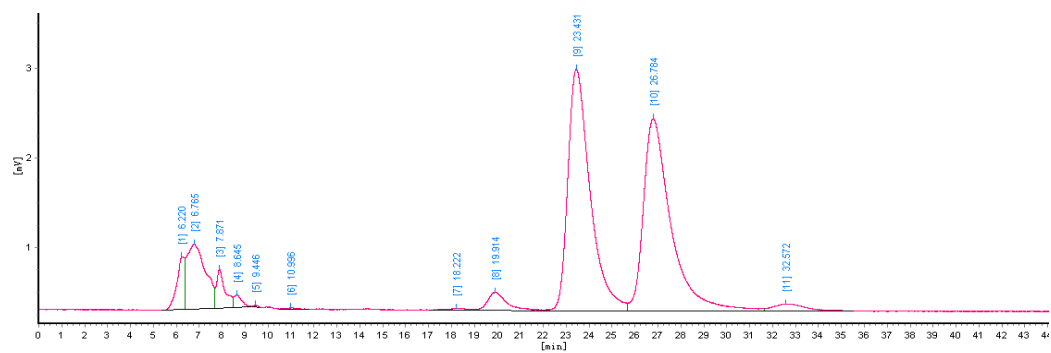


Figure S13. The chiral resolution HPLC spectra of compounds **1a/1b**.

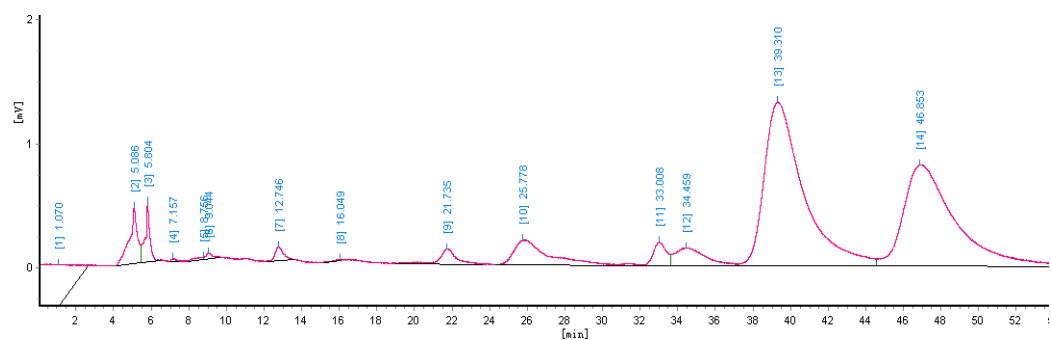


Figure S14. The chiral resolution HPLC spectra of compounds **2a/2b**.

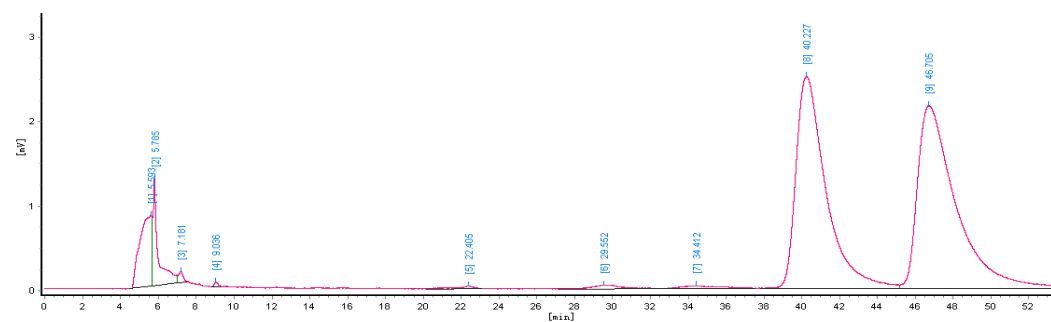


Figure S15. The chiral resolution HPLC spectra of compounds **3a/3b**.